p-type ZnS:N nanowires: Low-temperature solvothermal doping and optoelectronic properties

Ming-Zheng Wang, Wei-Jie Xie, Han Hu, Yong-Qiang Yu, Chun-Yan Wu, Li Wang, and Lin-Bao Luo

Citation: Applied Physics Letters **103**, 213111 (2013); doi: 10.1063/1.4833275
View online: http://dx.doi.org/10.1063/1.4833275
View Table of Contents: http://scitation.aip.org/content/aip/journal/apl/103/21?ver=pdfcov
Published by the AIP Publishing

Re-register for Table of Content Alerts

Create a profile.
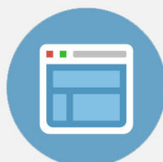
Sign up today!

This article is copyrighted as indicated in the article. Reuse of AIP content is subject to the terms at: http://scitation.aip.org/termsconditions. Downloaded to IP: 61.132.138.212 On: Thu, 09 Jan 2014 06:55:48

p-type ZnS:N nanowires: Low-temperature solvothermal doping and optoelectronic properties

Ming-Zheng Wang, Wei-Jie Xie, Han Hu, Yong-Qiang Yu, Chun-Yan Wu, Li Wang, and Lin-Bao Luo[a)]
School of Electronic Science and Applied Physics and Anhui Provincial Key Laboratory of Advanced Functional Materials and Devices, Hefei University of Technology, Hefei, Anhui 230009, People's Republic of China

(Received 17 September 2013; accepted 10 November 2013; published online 21 November 2013)

Nitrogen doped *p*-type ZnS nanowires (NWs) were realized using thermal decomposition of triethylamine at a mild temperature. Field-effect transistors made from individual ZnS:N NWs revealed typical *p*-type conductivity behavior, with a hole mobility of 3.41 $cm^2V^{-1}s^{-1}$ and a hole concentration of $1.67 \times 10^{17}\,cm^{-3}$, respectively. Further analysis found that the ZnS:N NW is sensitive to UV light irradiation with high responsivity, photoconductive gain, and good spectral selectivity. The totality of this study suggests that the solvothermal doping method is highly feasible to dope one dimensional semiconductor nanostructures for optoelectronic devices application. © *2013 AIP Publishing LLC*. [http://dx.doi.org/10.1063/1.4833275]

Zinc sulfide (ZnS), as one of the first semiconductors discovered, has already shown marvelous versatility and promise for novel and diverse applications, including light-emitting diodes (LEDs), flat panel display, electroluminescence, infrared windows sensors, lasers, and bio devices.[1–3] Compared with other popular and widely known semiconductors, such as ZnO and GaN nanowires (NWs), there are some unique properties exhibited in ZnS nanostructures. To name a few, ZnS has a large bandgap of 3.77 eV for the hexagonal wurtzite phase and 3.72 eV for the cubic phase at room temperature and accordingly, it is more suitable for ultraviolet (UV) light based devices, such as photodetectors.[4] But intrinsic ZnS in native forms is highly insulating due to its high crystal quality with little donor/acceptor defects and consequently, not suitable for device applications without doping.[5] As a result, the ability to dope ZnS NWs with suitable impurities, to achieve *n*-type or *p*-type conductivities, is highly desirable.

Nowadays, doping ZnS NWs with *n*- and *p*-type electrical conduction has been commonly achieved *via* an *in-situ* doping approach, which is simply to mix various dopants (such as Al,[6] Sb,[7] and Cu_2S (Ref. 8)) and ZnS powder or to introduce particular source gas (e.g., NH_3 (Ref. 9) when evaporating ZnS at high temperature. However, these methods often unavoidably involve using toxic chemicals or gases, and a high temperature, which limit the practical application of ZnS NWs. One possible solution to this issue is low-temperature hydrothermal or solvothermal approach. For example, recently, Yu *et al.* proposed a diethylenetriamine (DETA) assisted solvothermal method to achieve nitrogen-doped graphene. It was found that at solvothermal condition, DETA will decompose at the surface of graphene to emit nitrogen atoms, leading to the formation of nitrogen-doped graphene at a mild temperature.[10] Besides nitrogen, other species such as sulfur[11] and lanthanide atoms[12] can also be similarly incorporated at low temperature. Enlightened by the above, we, herein, present a facile and solvothermal method to dope ZnS NWs with nitrogen under a mild condition. The as-doped ZnS NWs exhibit typical *p*-type conductivity, with a hole concentration of $1.67 \times 10^{17}\,cm^{-3}$ and hole mobility of 3.41 $cm^2V^{-1}s^{-1}$. Besides, the nanostructure can be employed to fabricate UV photodetector with high responsivity and photoconductive gain. This method is probably suitable for other II–VI semiconductors, thus opening up the opportunities for a host of high-performance nanodevices based on *p*-type II–VI nanostructures.

The doping of ZnS NWs begins with the synthesis of intrinsic ZnS NWs. Briefly, thermal evaporation of ZnS powder onto a Si substrate coated with a Au catalyst was carried out in a horizontal quartz tube furnace, using high-purity argon premixed with 5% hydrogen as the carrier gas at 1040 °C for 2 h.[13] After cooling down, the white wool-like products were mixed with 10 ml triethylamine in a Teflon-lined stainless steel autoclave, followed by solvothermal treatment at 120 °C for 13 h. After that the obtained suspensions were taken out and cooled down to room temperature naturally. The yellow solid products were then collected by centrifuging the mixture, washed with deionized water and absolute ethanol for several times, and dried in a vacuum chamber for further characterization. The as-synthesized ZnS:N NWs were characterized by X-ray diffraction (XRD, Rigaku D/Max-rB), field-emission scanning electron microscopy (FE-SEM, SIRION 200 FEG), high-resolution transmission electron microscopy (HRTEM, Philips CM200 FEG), energy dispersive X-ray spectrometer (EDS) equipped in the TEM, and X-ray photoelectron spectrometer (XPS, Thermo ESCALAB 250). Room-temperature photoluminescence (RT-PL, LabRAM-HR) analysis was carried out by using He–Cd 325 nm laser as the excitation source. To assess the electrical transport properties of the ZnS:N NWs, back-gate FETs based on individual nanowires were constructed. The as-synthesized ZnS:N NWs were first dispersed on a SiO_2 (300 nm)/p^+-Si substrate, and then Cu/Au (10/50 nm) double-layer source and drain electrodes were defined by photolithography and lift-off processes, followed by electron beam evaporation. The Si substrate served as the global back

[a)]Author to whom correspondence should be addressed. Electronic mail: luolb@hfut.edu.cn

This article is copyrighted as indicated in the article. Reuse of AIP content is subject to the terms at: http://scitation.aip.org/termsconditions. Downloaded to IP: 61.132.138.212 On: Thu, 09 Jan 2014 06:55:48

gate. A fast annealing process in vacuum (5×10^{-4} Torr) at 300 °C for 3 min was carried out to further improve the electrical contact between the Cu/Au electrodes and the ZnS:N NWs. All the electrical and photoresponse properties were performed at room temperature using a semiconductor *I-V* characterization system (Keithley 4200-SCS).

Fig. 1(a) exhibits the schematic illustration of the preparation of ZnS:N NWs. Figs. 1(b) and 1(c) show the typical SEM and TEM images of the ZnS:N NWs with lengths of 400–600 μm, and a diameter of 80 to 100 nm. Compared with undoped ZnS NWs, it is found that the morphology of ZnS:N NWs remains unchanged. The inset of Fig. 1(c) depicts the EDS profile of ZnS:N NWs, revealing an approximate stoichiometric ratio of Zn: S ≈ 25:24. Further XRD patterns in Fig. 1(d) indicate that all of the diffraction peaks can be readily indexed to wurtzite structured ZnS, without any impurity and contaminant phases. The nearly identical XRD pattern after solvothermal treatment suggests that the incorporation of N atoms does not alter the lattice structure of the ZnS. The HRTEM image, combined with the selected-area electron diffraction (SAED) pattern in Fig. 1(e), shows that the ZnS: N NWs grow preferentially along [10$\bar{1}$0], in consistence with literature value.[8]

As often observed in ZnO,[14] TiO_2,[15] after nitrogen doping *via* solvothermal method, distinct color change from white to pale yellow was observed (Fig. 2(a)). Fig. 2(b) depicts the room-temperature PL spectra of both the ZnS:N NWs and undoped ones, from which it is seen that both of the samples consist a broad green emission at ~520 nm owing to the deep-level emission associated with the sulfur vacancies.[16,17] Besides, a weak emission band at 580 nm is also observed on the ZnS:N NW.[18] This emission peak is rarely reported and probably associated with the nitrogen doping. For the undoped ZnS NWs, an additional emission band at around 460 nm due to defect-related emission of ZnS host is observed.[19] The role of ZnS is mainly as a host, absorbing energy and transferring the excited electron to the dopants, from which the emission with various colors occurs. Accordingly, the defect-related emission of the ZnS host is weak and cannot be observed in the doped case.

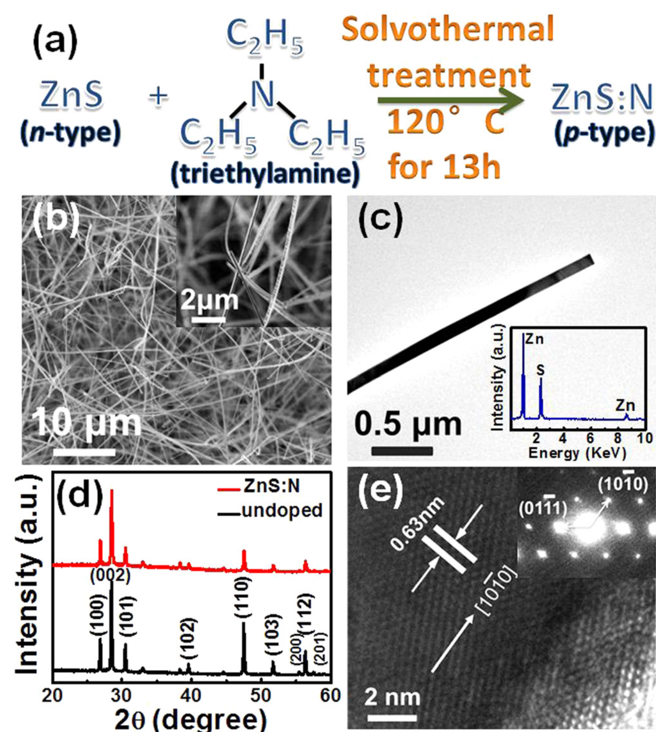

FIG. 1. (a) Schematic illustration of the preparation of ZnS:N NWs. (b) SEM image of the ZnS:N NWs, the inset is an SEM image at high magnification. (c) TEM image of the ZnS:N NW, the inset is the corresponding EDS spectrum. (d) XRD patterns of both undoped ZnS and nitrogen doped ZnS NWs. (e) HRTEM image of the ZnS:N NWs, the inset shows the corresponding SAED pattern.

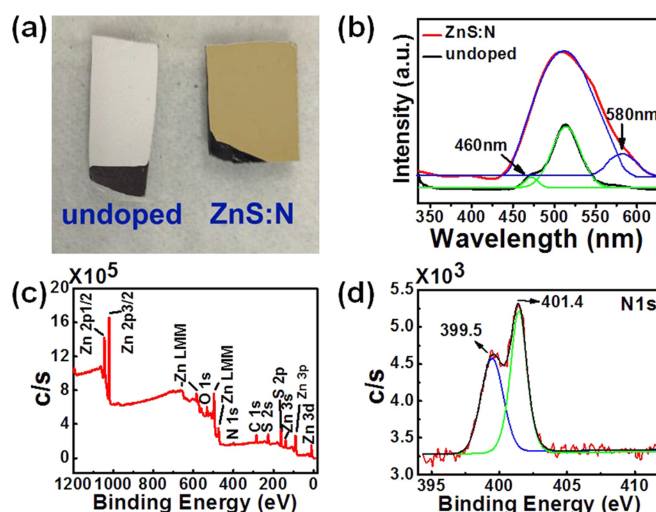

FIG. 2. (a) Photograph of both undoped and nitrogen doped ZnS NWs. (b) PL spectra of both undoped and nitrogen doped ZnS NWs. (c) XPS spectrum of ZnS:N NWs, the atomic percentage of N atoms is ~2.5%. (d) Corresponding high-resolution N1s spectrum.

XPS analysis was then performed to reveal the chemical environment and states of N in the ZnS:N NWs. As exhibited in Fig. 2(c), in addition to the Zn and S signals, a weak peak at around 400 eV corresponding to N1s core level is observed, suggesting that N atoms are indeed incorporated into the ZnS NWs. Fig. 2(d) shows the high-resolution N1s spectra, by decomposing the asymmetric line profile, two separate peaks centered at 399.5 and 401.4 eV are obtained, indicative of the presence of two kinds of N atoms with different chemical surrounding. The signal at low energy is probably ascribed to zinc nitride, in which the N atom has secured substantial charge from the surrounding metal atoms.[20] That is to say, the sites of sulfur atoms were replaced with nitrogen atoms in the ZnS. Moreover, the higher binding energy peak is attributed to N species with strong oxygen adsorption on the surface when the ZnS:N NWs is exposed to air.[21] The solvothermal doping mechanism can be understood as follows: At high pressure condition, like DETA,[10] the Et_3N molecules are highly unstable and apt to emit huge amount of N atoms which can either substitute the sites of sulfur anions in the ZnS lattice, giving rise to the formation of zinc nitride, or fill in the sulfur vacancies on the NW surface.[22] Owing to the huge surface to volume ratio, the nitrogen atoms on the nanostructures surface can be readily absorbed by ambient oxygen, which constitute the main reason for the Schottky junction.

To assess the effect of N doping on the electrical properties of the ZnS NWs, back-gate FETs were fabricated from individual NWs. According to the typical *I–V* curves of the

This article is copyrighted as indicated in the article. Reuse of AIP content is subject to the terms at: http://scitation.aip.org/termsconditions. Downloaded to IP: 61.132.138.212 On: Thu, 09 Jan 2014 06:55:48

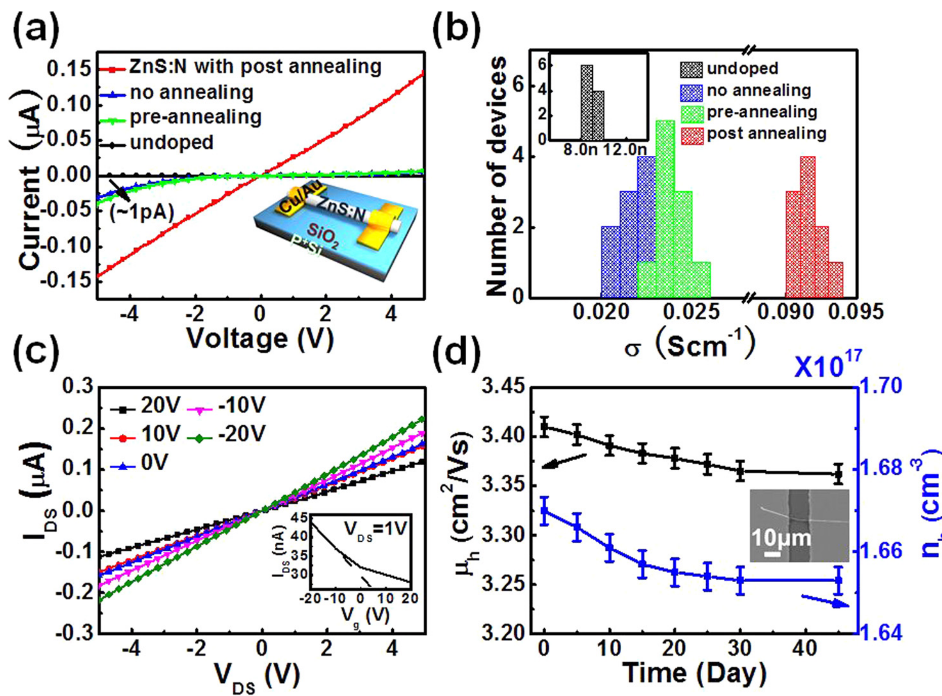

FIG. 3. (a) Typical I–V curves of undoped and N doped ZnS NWs under different annealing process; the inset shows the schematic illustration of the back-gate FET based on a single ZnS:N NW. (b) Distribution of conductivity for 40 devices, 10 devices each for the undoped ZnS, the doped ZnS without annealing, the ZnS with pre-annealing, and ZnS with post-annealing. (c) I_{DS}-V_{DS} plots of a FET made of an individual ZnS:N NW after post annealing, the inset exhibits typical transfer characteristics of the FET at $V_{DS} = 1$ V. (d) Hole mobility and concentration evolution of the ZnS:N NWs as a function of time. The inset is a typical SEM image of the FET.

samples in Fig. 3(a), the undoped ZnS NW exhibits an extremely low conductivity of less than 1×10^{-8} Scm^{-1}. By contrast, the conductivity is observed to dramatically increase by 7 orders of magnitude, to 9.2×10^{-2} Scm^{-1} after solvothermal doping. It should be noted that the sequence of annealing plays a vitally important role in determining the contact nature of the ZnS:N NW/Cu/Au: Annealing of ZnS:N NW prior to device fabrication can form Schottky junction to ZnS:N NW with obvious Schottky barrier (see the green line denoted as pre-annealing), while post-annealing, after device fabrication on the contrary, will lead to the formation of Ohmic contact. Such an improvement in contact is possibly due to the formation of highly conducting CuS film between the ZnS:N NW and Cu/Au electrode at high temperature.[23] Fig. 3(c) displays the source–drain current (I_{DS}) versus source–drain voltage (V_{DS}) curves at varied gate voltages (V_{GS}), exhibiting typical p-type gating effect. The hole mobility (μ_h) is estimated to be 3.41 cm^{2}V^{-1}s^{-1} at $V_{DS} = 1$ V and the hole concentration (n_h) is $\sim 1.67 \times 10^{17}$ cm^{-3}. The calculated hole mobility of the ZnS:N NWs is much higher than that of Sb-doped ZnS nanoribbons (NRs) (0.2 cm^{2}V^{-1}s^{-1}),[7] and nitrogen-doped ZnS NRs synthesized by applying ammonia gas as the acceptor source (0.2 cm^{2}V^{-1}s^{-1}), suggesting the high feasibility of the solvothermal strategy for semiconductors doping.[9] The above results indubitably demonstrate that efficient p-type doping in the ZnS NWs is accomplished by decomposing triethylamine molecules. To unveil the stability of the as-doped ZnS:N NWs, we then checked the evolution of both conductivity and hole mobility after long-term storage in drying cabinet (Fig. 3(d)). Apparently, one can see that the ZnS:N NWs experience a nominal decrease in hole mobility and concentration. This slight change in hole mobility and concentration (less than 1%) is probably associated with the increasing oxygen adsorption on N species at surface when exposed to ambient condition.

Next, we examined the optoelectronic property of the as-prepared ZnS:N NWs. As illustrated in Fig. 4(a), the ZnS:N NW shows a remarkable photocurrent (I_{light}/I_{dark} ratio $\sim$5 at a reverse bias of -5 V) when the device is exposed to 254 nm UV illumination. In addition, the ZnS:N NW device can be readily switched between high- and low-conduction states with good reproducibility when the UV light was alternatively turned on and off. To further evaluate the capability of this single ZnS:N NW based photodetector, we calculate the responsivity (R) and photoconductive gain (G) by the following equation:

$$R(\mathrm{A\,W^{-1}}) = I_P/P_{opt} = \eta(q\lambda/hc)G,$$

where I_P, P_{opt}, η, λ, h, and c are the photocurrent, the incident light power, the quantum efficiency, the light

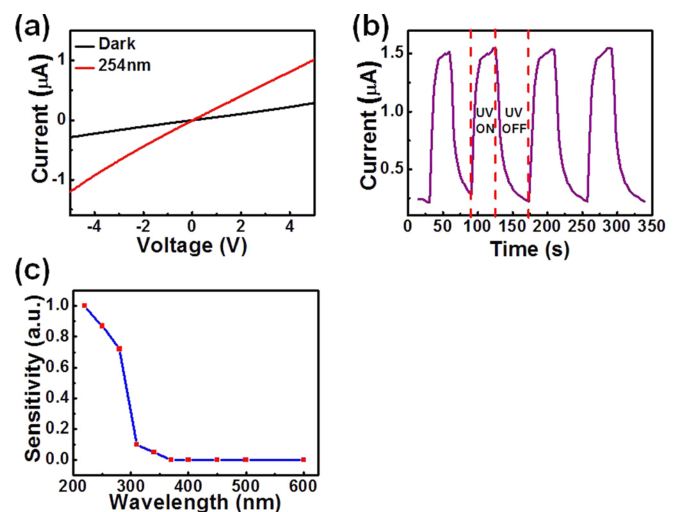

FIG. 4. (a) I–V curves of a single ZnS:N NW based UV photodetector with and without UV-light illumination, during testing the light intensity is kept at 20 μW cm^{-2}. (b) Photoresponse of the UV photodetector to pulsed UV-light (254 nm, 20 μW cm^{-2}) measured at an external applied bias of 5 V. (c) Spectral response of the ZnS:N NW based UV photodetector.

This article is copyrighted as indicated in the article. Reuse of AIP content is subject to the terms at: http://scitation.aip.org/termsconditions. Downloaded to IP: 61.132.138.212 On: Thu, 09 Jan 2014 06:55:48

TABLE I. Summary of the device performance of our UV photodetector and other UV photodetectors with similar device structures.

	R (A W^{-1})	G	t_r (s)	t_f (s)
ZnS:N NWs	1.4×10^5	7×10^5	36	51
ZnS:Al NRs[a]	8.8×10^5	4.3×10^6	95	209
ZnS:Cl NRs[b]	8.2×10^5	4.0×10^6	59	86
ZnO NRs[c]	/	$\sim10^2$	~100	~400
GaN NWs[d]	$\sim10^2$	$\sim10^2$	~100	~300

[a]See Ref. 6.
[b]See Ref. 26.
[c]See Ref. 27.
[d]See Ref. 28.

wavelength, the Planck's constant, and the light speed, respectively. R is estimated to be 1.43×10^5 A W^{-1} at a reverse bias of -5 V assuming $\eta = 1$ for simplification. Meanwhile, G is calculated to be 7×10^5. Notably, both R and G, corresponding to doped ZnS NW in this work, are comparable to that of n-type ZnS NWs photodetector, but much higher than that of ZnO and GaN nanostructures based devices (Table I). This relatively high R and G can be related to the presence of defect states in ZnS:N NWs. Once the device is illuminated with UV light, the states caused by nitrogen doping will function also as effective trapping states.[24] By lessening the electron–hole recombination (trapping the minority carriers (electrons)), the lifetime of the photocarriers is considerably prolonged.[25] Apart from the high responsivity and gain, the ZnS:N NW exhibits a good spectral selectivity. Fig. 4(c) plots the normalized responsivity of the UV photodetector as a function of wavelength. The conductance of the ZnS:N NWs strongly depends on the light wavelength with the cut-off wavelength of ~330 nm, which is consistent with the bandgap of ZnS. This finding signifies that the increase of the photocurrent is mainly due to the electron–hole pairs excited by the incident light with energy greater than the bandgap.

In conclusion, we have demonstrated an effective approach to the synthesis of *p*-type ZnS:N NWs doping *via* a low-temperature triethylamine decomposition method. The as-doped ZnS NW exhibits typical *p*-type conduction behavior, with a hole concentration of 1.67×10^{17} cm^{-3} and hole mobility of 3.41 cm^{2}V^{-1}s^{-1}, respectively. In addition, the UV photodetector constructed from the single ZnS:N NW exhibits excellent device performance, in terms of high responsivity and photoconductive gain. This study corroborates that such a solvothermal doping scheme by triethylamine decomposition has great potential for future optoelectronic devices application.

This work was supported by the National Natural Science Foundation of China (NSFC, Nos. 61106010, 21101051) and the Fundamental Research Funds for the Central Universities (Nos. 2013HGXJ0195, 2013HGCH0012).

[1]M. Bredol and J. Merikhi, J. Mater. Sci. **33**, 471 (1998).
[2]T. Yamamoto, S. Kishimoto, and S. Iida, Physica B **308–310**, 916 (2001).
[3]X. S. Fang, Y. Bando, M. Liao, U. K. Gautam, C. Zhi, B. Dierre, B. Liu, T. Zhai, T. Sekiguchi, Y. Koide, and D. Golberg, Adv. Mater. **21**, 2034 (2009).
[4]X. S. Fang, T. Zhai, U. K. Gautam, L. Li, L. Wu, Y. Bando, and D. Golberg, Prog. Mater. Sci. **56**, 175 (2011).
[5]Y. Q. Yu, L. B. Luo, Z. F. Zhu, B. Nie, Y. G. Zhang, L. H. Zeng, Y. Zhang, C. Y. Wu, L. Wang, and Y. Jiang, CrystEngComm **15**, 1635 (2013).
[6]P. Jiang, J. S. Jie, Y. Q. Yu, Z. Wang, C. Xie, X. W. Zhang, C. Y. Wu, L. Wang, Z. F. Zhu, and L. B. Luo, J. Mater. Chem. **22**, 6856 (2012).
[7]Q. Peng, J. S. Jie, C. Xie, L. Wang, X. W. Zhang, D. Wu, Y. Q. Yu, C. Y. Wu, Z. Wang, and P. Jiang, Appl. Phys. Lett. **98**, 123117 (2011).
[8]Y. Q. Yu, Y. Jiang, P. Jiang, Y. G. Zhang, D. Wu, Z. F. Zhu, Q. Liang, S. R. Chen, Y. Zhang, and J. S. Jie, J. Mater. Chem. C **1**, 1238 (2013).
[9]G. D. Yuan, W. J. Zhang, W. F. Zhang, X. Fan, I. Bello, C. S. Lee, and S. T. Lee, Appl. Phys. Lett. **93**, 213102 (2008).
[10]P. Chen, T. Y. Xiao, H. H. Li, J. J. Yang, Z. Wang, H. B. Yao, and S. H. Yu, ACS Nano **6**, 712 (2012).
[11]Z. X. Zhao, H. X. Dai, J. G. Deng, Y. X. Liu, and C. T. Au, Chin. J. Catal. **34**, 1617 (2013).
[12]R. X. Yan and Y. D. Li, Adv. Funct. Mater. **15**, 763 (2005).
[13]M. Y. Lu, L. J. Chen, W. J. Mai, and Z. L. Wang, Appl. Phys. Lett. **93**, 242503 (2008).
[14]X. Yang, A. Wolcott, G. Wang, A. Sobo, R. C. Fitzmorris, F. Qian, J. Z. Zhang, and Y. Li, Nano Lett. **9**, 2331 (2009).
[15]R. Asahi, T. Morikawa, T. Ohwaki, K. Aoki, and Y. Taga, Science **293**, 269 (2001).
[16]X. H. Zhang, Y. Zhang, Y. P. Song, Z. Wang, and D. P. Yu, Physica E (Amsterdam) **28**, 1 (2005).
[17]P. Prathap, N. Revathi, Y. P. V. Subbaiah, K. T. Ramakrishna Reddy, and R. W. Miles, Solid State Sci. **11**, 224 (2009).
[18]S. C. Qu, W. H. Zhou, F. Q. Liu, N. F. Chen, Z. G. Wang, H. Y. Pan, and D. P. Yu, Appl. Phys. Lett. **80**, 3605 (2002).
[19]Y. C. Zhu, Y. Bando, and D. F. Xue, Appl. Phys. Lett. **82**, 1769 (2003).
[20]K. Toyoura, H. Tsujimura, T. Goto, K. Hachiya, R. Hagiwara, and Y. Ito, Thin Solid Films **492**, 88 (2005).
[21]J. M. Bian, X. M. Li, X. D. Gao, W. D. Yu, and L. D. Chen, Appl. Phys. Lett. **84**, 541 (2004).
[22]R. A. Street and N. F. Mott, Phys. Rev. Lett. **35**, 1293 (1975).
[23]Y. Q. Yu, L. H. Zeng, Y. Jiang, and J. S. Jie, IEEE Electron Device Lett. **34**, 810 (2013).
[24]G. Cheng, X. Wu, B. Liu, B. Li, X. Zhang, and Z. Du, Appl. Phys. Lett. **99**, 203105 (2011).
[25]C. Soci, A. Zhang, B. Xiang, S. A. Dayeh, D. P. R. Aplin, J. Park, X. Y. Bao, Y. H. Lo, and D. Wang, Nano Lett. **7**, 1003 (2007).
[26]Y. Q. Yu, J. S. Jie, X. W. Zhang, L. Wang, C. Wu, Q. Peng, X. Zhang, Z. Wang, C. Xie, D. Wu, and Y. Jiang, J. Mater. Chem. **21**, 12632 (2011).
[27]Y. K. Su, S. M. Peng, L. W. Ji, C. Z. Wu, W. B. Cheng, and C. H. Liu, Langmuir **26**, 603 (2010).
[28]R. Calarco, M. Marso, T. Richter, A. I. Aykanat, R. Meijers, A. v. d. Hart, T. Stoica, and H. Lüth, Nano Lett. **5**, 981 (2005).

This article is copyrighted as indicated in the article. Reuse of AIP content is subject to the terms at: http://scitation.aip.org/termsconditions. Downloaded to IP: 61.132.138.212 On: Thu, 09 Jan 2014 06:55:48